NACA RM A55B14

RESEARCH MEMORANDUM

WIND-TUNNEL INVESTIGATION AT LOW SPEED OF A WING HAVING 63° SWEEPBACK AND A DROOPED TIP

By James R. Blackaby

Ames Aeronautical Laboratory
Moffett Field, Calif.

CLASSIFICATION CHANGED

To UNCLASSIFIED

By authority of Navy Res. ltr. 4RN-112 Date 2-15-57
NACA 3-13-57

NATIONAL ADVISORY COMMITTEE
FOR AERONAUTICS

WASHINGTON

April 7, 1955

[redacted]L

NACA RM A55B14

NATIONAL ADVISORY COMMITTEE FOR AERONAUTICS

RESEARCH MEMORANDUM

WIND-TUNNEL INVESTIGATION AT LOW SPEED OF A WING HAVING 63° SWEEPBACK AND A DROOPED TIP

By James R. Blackaby

SUMMARY

The results of force tests made at low speed are presented to show the effect on longitudinal static stability produced by drooping the tip of a 63° sweptback wing. Five semispan wing models were tested: two incorporating curved drooped tips, two with abruptly drooped tips, and one without droop. In addition, the effects of fences and of a leading-edge flap on the outer portion of the wing were investigated. Curved droop was found to have no beneficial effect on the stability of the wing; whereas abrupt droop was found to produce an improvement comparable to that attained with a fence on the undrooped wing. The most favorable stability characteristics were measured for a model with an abruptly drooped tip, a fence, and a leading-edge flap; however, the use of these same auxiliary devices on the undrooped wing was nearly as effective.

INTRODUCTION

Low-speed tests (refs. 1 and 2) have shown a 63° sweptback wing to possess undesirable longitudinal-stability characteristics exemplified by large variations of stability for lift coefficients greater than about 0.3. The cause of these stability variations can be traced to changes in lift at sections near the wing tip as a result of local stall. Improvements of the stability characteristics of 63° sweptback wings have been effected by the use of fences and auxiliary lift devices as in reference 1, and by twisting and cambering the wing as in reference 3. In all cases, the purpose of the modifications was to increase the lift capabilities of the tip portions of the wing.

It has been proposed that the use of large amounts of negative dihedral of the outer portions of the sweptback wing might sufficiently alter the spanwise flow of boundary-layer air, as well as decrease the local angle of attack of these sections, in such a manner as to effect some further improvement in the stability of the wing. To check this

hypothesis, the investigation reported herein included tests of a semispan wing with the outer portion curved downward in an arc (curved-droop model). In addition, tests were made of a semispan wing with the tip portion drooped abruptly (abrupt-droop model) to find the extent to which the discontinuity would affect the stability characteristics. Tests were also made with fences and with a leading-edge flap on the outer portion of an undrooped and an abruptly drooped wing to provide a comparison of the effects of these devices with the effect of droop in improving the stability characteristics of the 63° sweptback wing.

The tests reported were conducted in one of the Ames 7- by 10-foot wind tunnels at a Reynolds number of 3,700,000 based on the mean aerodynamic chord.

NOTATION

b	span of semispan wing, perpendicular to the plane of symmetry (fig. 1)
C_D	drag coefficient, $\frac{\text{drag}}{qS}$
C_L	lift coefficient, $\frac{\text{lift}}{qS}$
C_m	pitching-moment coefficient, $\frac{\text{pitching moment}}{qS}$
$c.p._b$	spanwise distance from the plane of symmetry to the center of pressure, measured perpendicular to the plane of symmetry, in terms of projected span, $\frac{\text{spanwise distance}}{b}$
$c.p._c$	chordwise distance from the leading edge of the mean aerodynamic chord to the center of pressure, in terms of the mean aerodynamic chord, $\frac{\text{chordwise distance}}{\bar{c}}$
c	wing chord, parallel to the plane of symmetry
$\bar{c}$	mean aerodynamic chord, $\frac{\int_0^b c^2 dy}{\int_0^b c\, dy}$, (fig. 1)
D	drag
h	vertical displacement of the mean aerodynamic chord from the chord plane of the basic wing (fig. 1)
L	lift

q	free-stream dynamic pressure, $\frac{1}{2}\rho V^2$
S	projected area of semispan wing (fig. 1)
s	chordwise distance from the leading edge of the root chord to the leading edge of the mean aerodynamic chord (fig. 1)
t	wing thickness
V	free-stream velocity
X	chordwise distance from the leading edge of the mean aerodynamic chord to the moment center (fig. 1)
x	distance from the center of pitch rotation of the model to the 0.25 point of the mean aerodynamic chord, positive to the rear (fig. 1)
y	spanwise station, measured perpendicular to the plane of symmetry
$y_{\bar{c}}$	distance from the plane of symmetry to the mean aerodynamic chord, measured perpendicular to the plane of symmetry (fig. 1)
α	angle of attack
ρ	mass density of air

MODEL DESCRIPTION

The models tested (fig. 1) were developed from two basic, undrooped, semispan wing designs, both having a leading-edge sweepback of 63° and the NACA 64A006 profile parallel to the plane of symmetry. The curved-droop models were developed from a basic wing having a semispan of 61.13 inches, a taper ratio of 0.246, and an aspect ratio (based on a complete wing) of 3.53. The abrupt-droop models were developed from a basic wing having a semispan of 60.00 inches, a taper ratio of 0.250, and an aspect ratio (based on a complete wing) of 3.50. The models were constructed of laminated mahogany glued to a 1/2-inch-thick steel-plate spar.

For the curved-droop models, the outer 36 inches of the semispan wing (approximately the outer 60 percent) was curved downward so that the slope of a tangent to the wing chord surface at the tip was -45° with respect to the inner, undrooped portion. The radius of curvature of the drooped portion (measured to the wing-chord surface) was 45.84 inches. Two curved-droop models were tested, one with a dihedral of 0° and the

[redacted]

other with a dihedral of 13°8', measured to the chord plane of the inner portion of the wing. The dihedral of 13°8' raised the tip chord to the level of the root chord.

For the abrupt-droop models, the outer 24 inches (outer 40 percent of the semispan) was drooped 40° for one model and 60° for another, with respect to the inner portion of the wing. The dihedral of the inner portion was constant at 15°. A third model of this series was tested with the outer portion undrooped. The 15° dihedral was incorporated to limit the displacement of the tip from the level of the root chord.

In the remainder of the report, the five models tested will be designated by numbers referring, respectively, to the inner dihedral and the outer droop. Thus, the curved-droop models are designated 0-45 and 13-45, while the abrupt-droop models are designated 15-0, 15-40, and 15-60. The pertinent dimensions of the models are tabulated in figure 1 and photographs of the models in the wind tunnel are shown in figure 2.

All the models were tested with the short fuselage used in the tests reported in reference 1. The coordinates of this fuselage are listed in table I, and the fuselage position, relative to that of the wing, is shown in figure 1. The method of installing the fuselage required that it be moved 1.50 inches from the center of rotation when it was used with the wings having 13°8' and 15° dihedral.

Two fences and a leading-edge flap were tested on models 15-0 and 15-40. (See fig. 3.) The fences were on the upper surface of the wing at about 60 percent of the semispan (just in from the droop discontinuity); one, designated the low fence, had a height equal to the wing thickness at 60 percent of the semispan, while the other, designated the high fence, had a height equal to three times the wing thickness. The leading-edge flap was applied only to the tip portion of the wing and had a chord equal to 15 percent of the wing chord. It was deflected 40°, measured in a plane perpendicular to the wing leading edge. This is the same flap that was used in the tests reported in reference 1, in which a deflection of 40° was stated to be optimum.

TESTS AND CORRECTIONS

The tests reported herein were made at a dynamic pressure of 40 pounds per square foot, which corresponded to a Reynolds number of about 3,700,000 based on the mean aerodynamic chord. In addition to lift and drag, measurements were made of the rolling moments about the root chord to permit the calculation of the spanwise location of the center of pressure.

The following equations, developed in reference 1, were considered to be sufficiently accurate for the correction of the data of the present investigation for wind-tunnel-wall effects:

$$C_D = C_{D_u} + 0.0319\, C_{L_u}^2$$

$$C_L = 0.99\, C_{L_u}$$

$$C_m = C_{m_u} + 0.0010\, C_{L_u}$$

$$\alpha = \alpha_u + 1.36 \left(C_{L_u}\right)_{w+f} + 0.19 \left(C_{L_u}\right)_w$$

The subscripts signify

u uncorrected

w wing

f flap

No corrections were applied to the rolling-moment data.

Measurements of the geometric deflection and twist of the models indicated that the maximum distortion occurred with the curved-droop models (0-45 and 13-45) at lift coefficients of 0.5 to 0.6. For these models the maximum deflection was about 3 inches at the tip and the twist reduced the angle of attack at the tip by about 1°. No corrections were applied to compensate for these distortions.

A gap of about 1/4 inch existed between the fuselage and the wind-tunnel floor and turntable. This was as small a gap as was practical and no corrections were applied for the effects of leakage.

Pitching moments were computed about a fixed axis (with respect to the axis of rotation of the models) which passed through the 0.25 point of the mean aerodynamic chord of model 0-45 (see fig. 1). For all the other models, the 0.25 points of the mean aerodynamic chords were to the rear of, and above, the moment axis. The pertinent dimensions are tabulated in figure 1.

[redacted]

RESULTS AND DISCUSSION

The lift, drag, and pitching-moment characteristics are shown in figure 4 for models 0-45 and 13-45, and in figure 5 for models 15-0, 15-40, and 15-60. Included in these figures are the characteristics of the wing and fuselage presented in reference 1 for a Reynolds number of 4,200,000. (In the nomenclature of the present report, the model of reference 1 would be designated 0-0.) It can be seen that drooping the wing tip, or incorporating dihedral, as was done in the present investigation, produced only small effects on the total-lift characteristics of the models (figs. 4(a) and 5(a)).

The pitching-moment characteristics presented in figure 4(a) show that the curved droop had only a small effect on the static longitudinal stability of the 63° sweptback wing. The failure of the drooped portion to promote an improvement of the stability characteristics in the manner proposed in the Introduction is thought to stem from the probability that an angle of droop great enough to be effective may not have been realized except near the extreme wing tip. The use of abrupt droop (fig. 5(a)) resulted in an improvement of the longitudinal-stability characteristics to the extent that the unstable reversal of the pitching-moment curve was delayed to higher lift coefficients. (The reasons for this improvement will be discussed later in the report.) The differences in slopes of the pitching-moment curves for the various models at low lift coefficients were due, primarily, to the physical displacement of the wing with respect to the moment center, a measure of which is the movement of the 0.25 point of the mean aerodynamic chord (tabulated on fig. 1).

An analysis of the drag characteristics of the models (figs. 4(b) and 5(b)) on the basis of the lift-drag ratios indicates that the effect of the curved droop was to increase the maximum L/D, while the effect of dihedral was to decrease it. As a result, the maximum lift-drag ratios for the curved-droop models and the wing of reference 1 (12.2 to 12.6) are higher than those for the 15° dihedral models (10.8 to 11.3).

Curves showing the chordwise and spanwise movement of the center of pressure on the models as a function of lift coefficient are presented in figure 6. (The scales used for chordwise and spanwise centers of pressure are proportional to the mean aerodynamic chord and span, respectively, of the individual models. Thus, the center-of-pressure movement shown by the curves of $c.p._b$ vs. $c.p._c$ is a true representation based on the projected plan forms of the models.) Two main features are shown by these curves: first, the comparatively small extent of the center-of-pressure movement for all the models in relation to the wing area (as shown by the sketch in the figure); and, second, the reduction in chordwise center-of-pressure movement for the 15° dihedral models, as the abrupt droop was increased to 40° and 60°. The range of center-of-pressure movement for

lift coefficients up to 0.75 was reduced from about 22 percent of the mean aerodynamic chord for model 15-0 to 16 and 5 percent for models 15-40 and 15-60, respectively.

The effects of the fences and of the leading-edge flap on the lift, drag, and pitching-moment characteristics are shown in figure 7 for model 15-0, and in figure 8 for model 15-40. It can be seen in figures 7(a) and 8(a) that the addition of these devices produced only small effects on the lift characteristics. The stability characteristics were altered considerably, however.

A comparison of the pitching-moment-coefficient curves in figures 5(a), 7(a), and 8(a) shows that the stability characteristics at medium to high lift coefficients were improved both by increasing the angle of abrupt droop and by adding a fence on the upper surface of the wing. The fact that the characteristics of model 15-0 with the high fence were similar to those of model 15-60 without a fence indicates that the discontinuity on the upper surface of the abruptly drooped models may have acted in the nature of a fence in increasing the lift of the tip portion of the wing. This increase in the lift capabilities of sections of a sweptback wing beyond a fence is probably due to a form of boundary-layer-control action similar to that which occurs for the portions near the root.

The addition of the leading-edge flap to model 15-0, without a fence, can be seen to have improved the stability characteristics for lift coefficients from about 0.25 to 0.45 (fig. 7(a)). The improvement in this lift range is attributed to a delay of the initial flow separation from the tip portion of the wing, resulting in a lower drag than was measured for the plain wing (fig. 7(b)). The addition of the leading-edge flap to model 15-40 resulted in a similar improvement of the stability characteristics for lift coefficients from about 0.30 to 0.65 (fig. 8(a)); up to the highest test lift coefficient, the combined effects of the leading-edge flap and the abrupt droop prevented the sharp unstable reversal of the pitching moments which occurred for the plain wing. The addition of the leading-edge flap and the high fence to model 15-40 resulted in the best stability characteristics measured for the models of the present investigation, although they were closely matched by the characteristics of model 15-0 with the same devices (up to a lift coefficient of about 0.83, where an abrupt loss of stability occurred for model 15-0), and of model 15-40 with the low fence and the leading-edge flap (figs. 7(a) and 8(a)).

The drag characteristics for models 15-0 and 15-40 with the fences and the leading-edge flap are presented in figures 7(b) and 8(b). For both models it can be seen that the addition of the high fence reduced the maximum L/D; whereas, the addition of the flap had only a small effect on the maximum L/D but increased the lift coefficient associated with it. The addition of both the high fence and the leading-edge flap produced a combination of these two effects, namely a reduction of

[redacted]

maximum L/D with an increase in the corresponding lift coefficient. The addition of the low fence to model 15-40 with the flap had only a small effect on L/D.

The curves presented in figures 7(c) and 8(c) show how the movements of the centers of pressure for models 15-0 and 15-40 were affected by the addition of the auxiliary devices. It can be seen that either of the fences, in combination with the leading-edge flap, was quite effective in reducing the center-of-pressure movement, especially in the chordwise direction. In the following table, the center-of-pressure movements are shown for models 15-0 and 15-40 with and without the leading-edge flap and fences for lift coefficients up to 0.75. The reduction of center-of-pressure movement and the similarity of stability characteristics for the models with the auxiliary devices are evident.

Model	Center-of-pressure movement, percent $\bar{c}$
15-0	22
15-0 + high fence + flap	4
15-40	16
15-40 + high fence + flap	3
15-40 + low fence + flap	5

CONCLUSIONS

Wind-tunnel tests at low speeds of the effects of drooped tips on the aerodynamic characteristics of a 63° sweptback semispan wing have shown that:

1. Abruptly drooping the outer 40 percent of the wing to angles of 40° and 60° caused an improvement in the stability characteristics of the wing. The chordwise center-of-pressure movement for lift coefficients up to 0.75 was reduced from 22 percent of the mean aerodynamic chord for an undrooped wing to 16 percent and 5 percent for 40° and 60° drooped-tip models, respectively. The improvement is thought to have resulted because the discontinuity accompanying the abrupt droop acted in the nature of a fence, causing some alteration of the spanwise flow of the boundary layer and an increase of the lift over the tip portion of the wing.

2. The best stability characteristics attained, utilizing a 40° abruptly drooped tip with an upper-surface fence and a leading-edge flap on the drooped portion of the wing, were very little better than could

[redacted]

be attained utilizing the same auxiliary devices on the wing without a drooped tip. For lift coefficients up to 0.75, the range of the chordwise center-of-pressure movement for the undrooped wing was reduced from 22 percent to about 4 percent of the mean aerodynamic chord by the addition of the leading-edge flap and the fence. For the wing with the 40° abruptly drooped tip, the addition of these devices reduced the center-of-pressure movement from about 16 percent to as little as 3 percent of the mean aerodynamic chord.

3. Curving the outer 60 percent of the wing downward was not effective in improving the stability characteristics of the wing.

Ames Aeronautical Laboratory
National Advisory Committee for Aeronautics
Moffett Field, Calif., Feb. 14, 1955.

REFERENCES

1. Hopkins, Edward J.: Aerodynamic Study of a Wing-Fuselage Combination Employing a Wing Swept Back 63°.- Effects of Split Flaps, Elevons, and Leading-Edge Devices at Low Speed. NACA RM A9C21, 1949.

2. McCormack, Gerald M., and Walling, Walter C.: Aerodynamic Study of a Wing-Fuselage Combination Employing a Wing Swept Back 63°.- Investigation of a Large-Scale Model at Low Speeds. NACA RM A8D02, 1948.

3. Weiberg, James A., and Carel, Hubert C.: Wind-Tunnel Investigation at Low Speed of a Wing Swept Back 63° and Twisted and Cambered for a Uniform Load at a Lift Coefficient of 0.5. NACA RM A50A23, 1950.

TABLE I.- COORDINATES OF THE FUSELAGE
[All dimensions in inches]

Station	Diameter	Station	Diameter
0	0	81.6	16.32
4	2.84	91.8	16.20
8	5.34	102.0	15.82
12	7.50	112.2	15.20
16	9.30	122.4	14.28
20	10.80	132.6	13.26
24	11.98	142.8	11.68
28	12.88	153.0	9.86
30.6	13.26	163.2	7.58
40.8	14.28	164.4	7.16
51.0	15.20	166.4	5.82
61.2	15.82	168.4	3.58
71.4	16.20	170.4	0

Fineness ratio, $\frac{\text{length}}{\text{maximum diameter}} = 10.4$

[redacted]

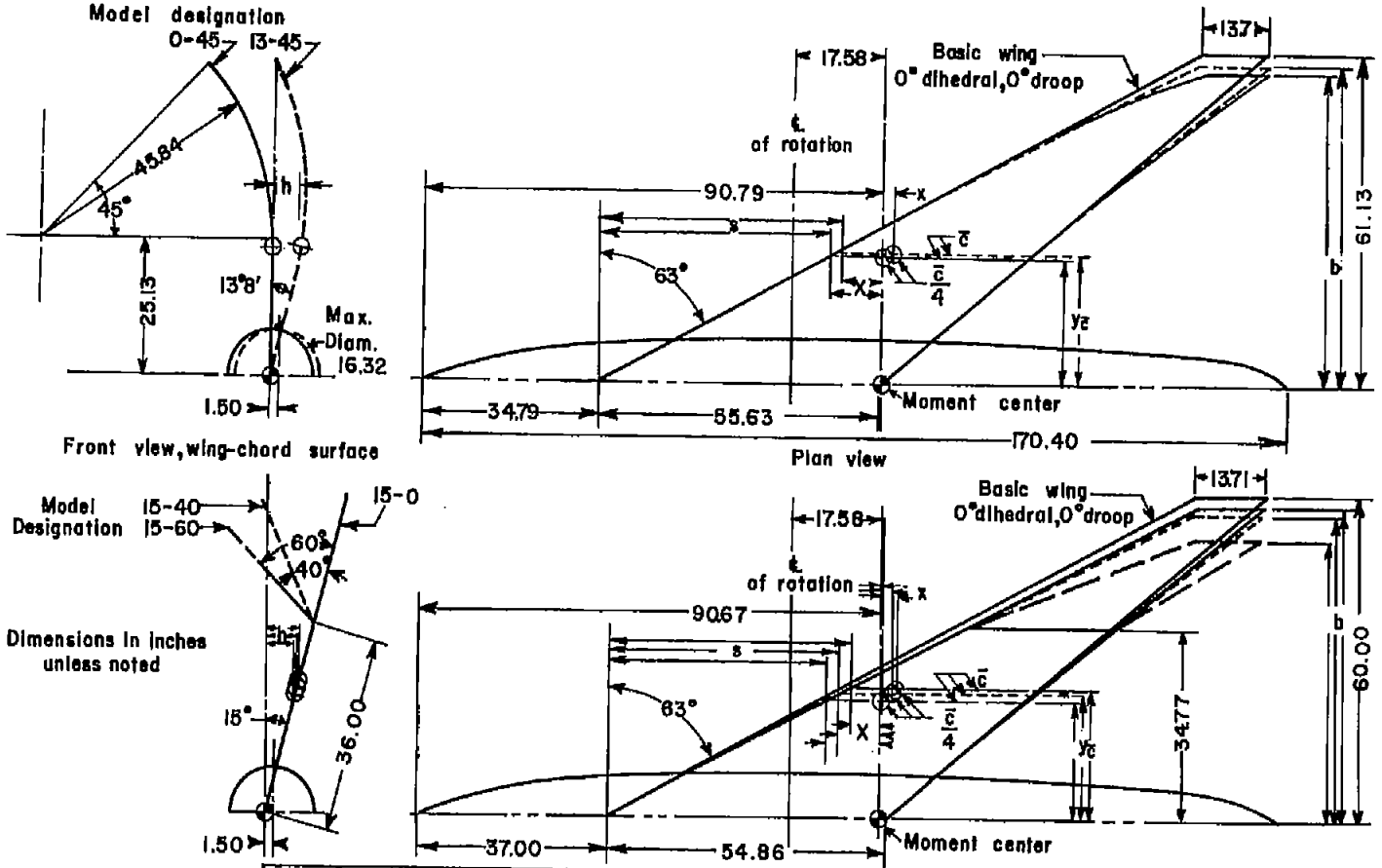

Model	b	Area, sq.ft.	c̄	c̄/4	X/c̄	x/c̄	h/c̄	yc̄/b	s
0-45	57.54	14.22	39.51	9.88	0.250	0	0	0.408	46.12
13-45	59.08	14.32	39.00	9.75	0.215	0.035	0.141	0.400	47.61
15-0	57.96	13.80	38.39	9.60	0.171	0.079	0.162	0.403	47.09
15-40	56.52	13.58	38.64	9.66	0.189	0.061	0.158	0.407	46.39
15-60	51.74	12.85	39.53	9.88	0.249	0.001	0.146	0.420	43.84

Figure 1.- Model details.

A-19097

(a) Model 13-45.

A-19477

(b) Model 15-0.

Figure 2.- Model photographs.

A-19480

(c) Model 15-40.

A-19488

(d) Model 15-60.

Figure 2.- Concluded.

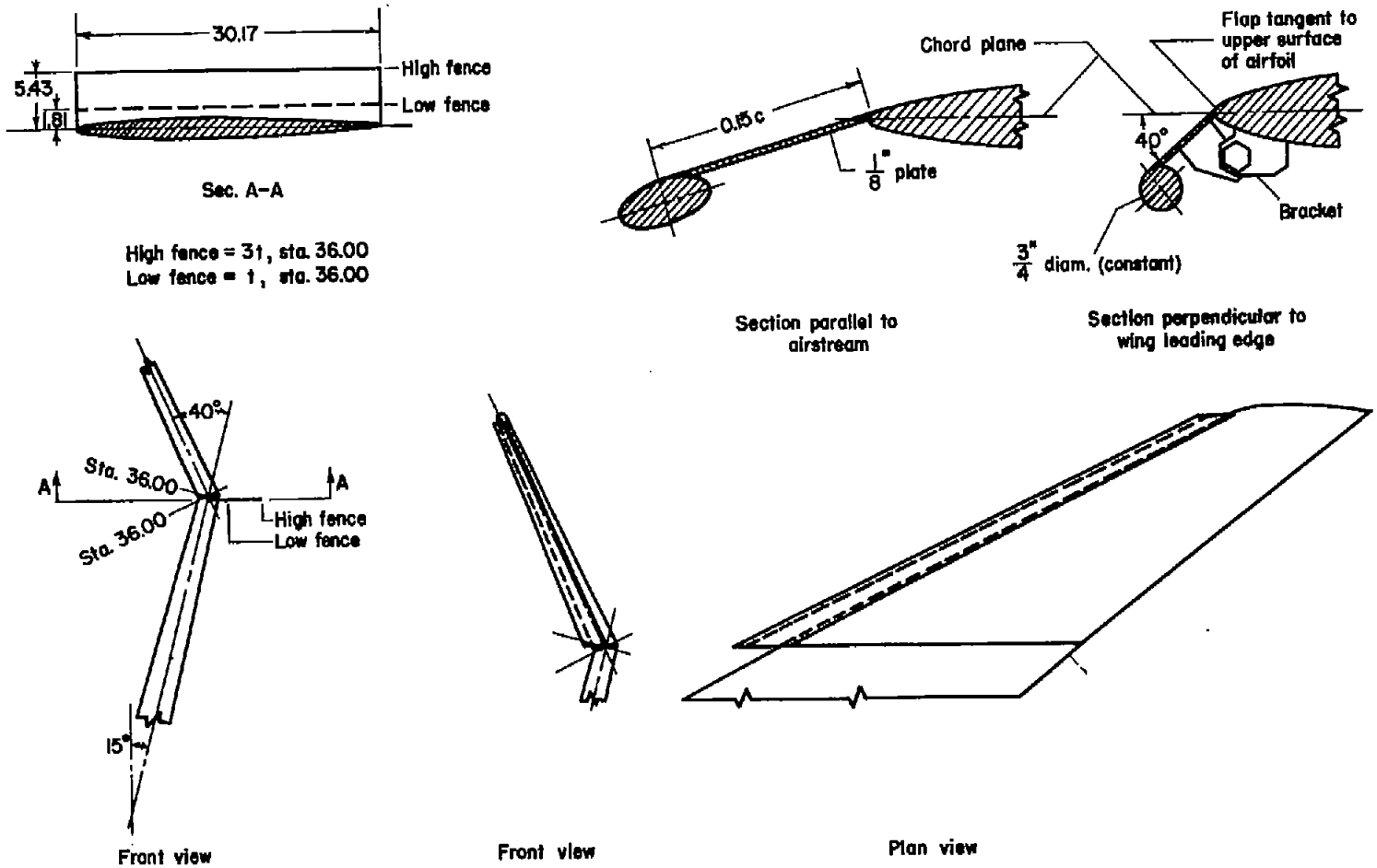

(a) Fence.

(b) Leading-edge flap.

Figure 3.- Upper-surface fence and leading-edge flap details.

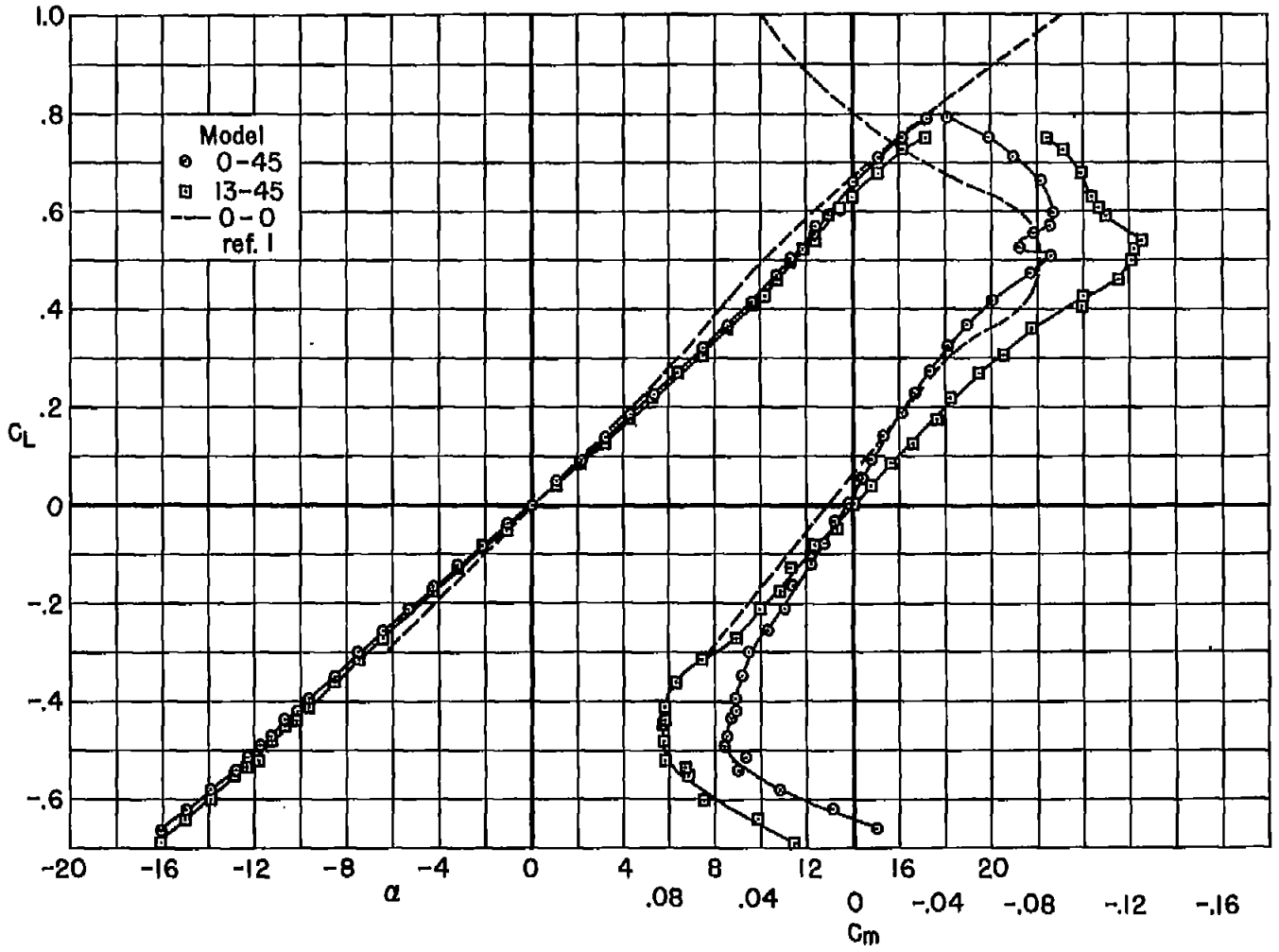

(a) Lift and pitching moment.

Figure 4.- Lift, pitching-moment, and drag characteristics of the curved-droop models.

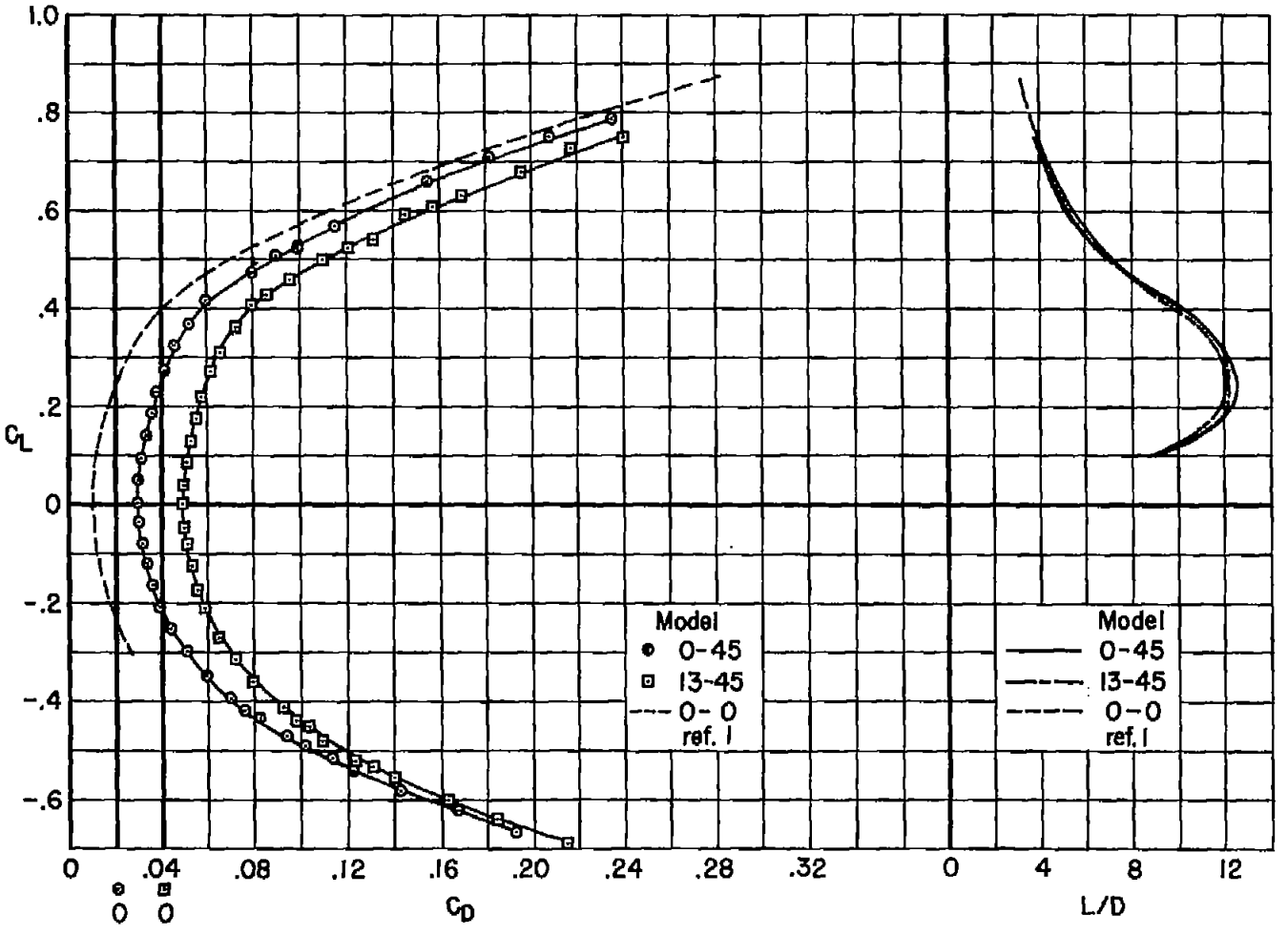

(b) Drag and lift-drag ratio.

Figure 4.- Concluded.

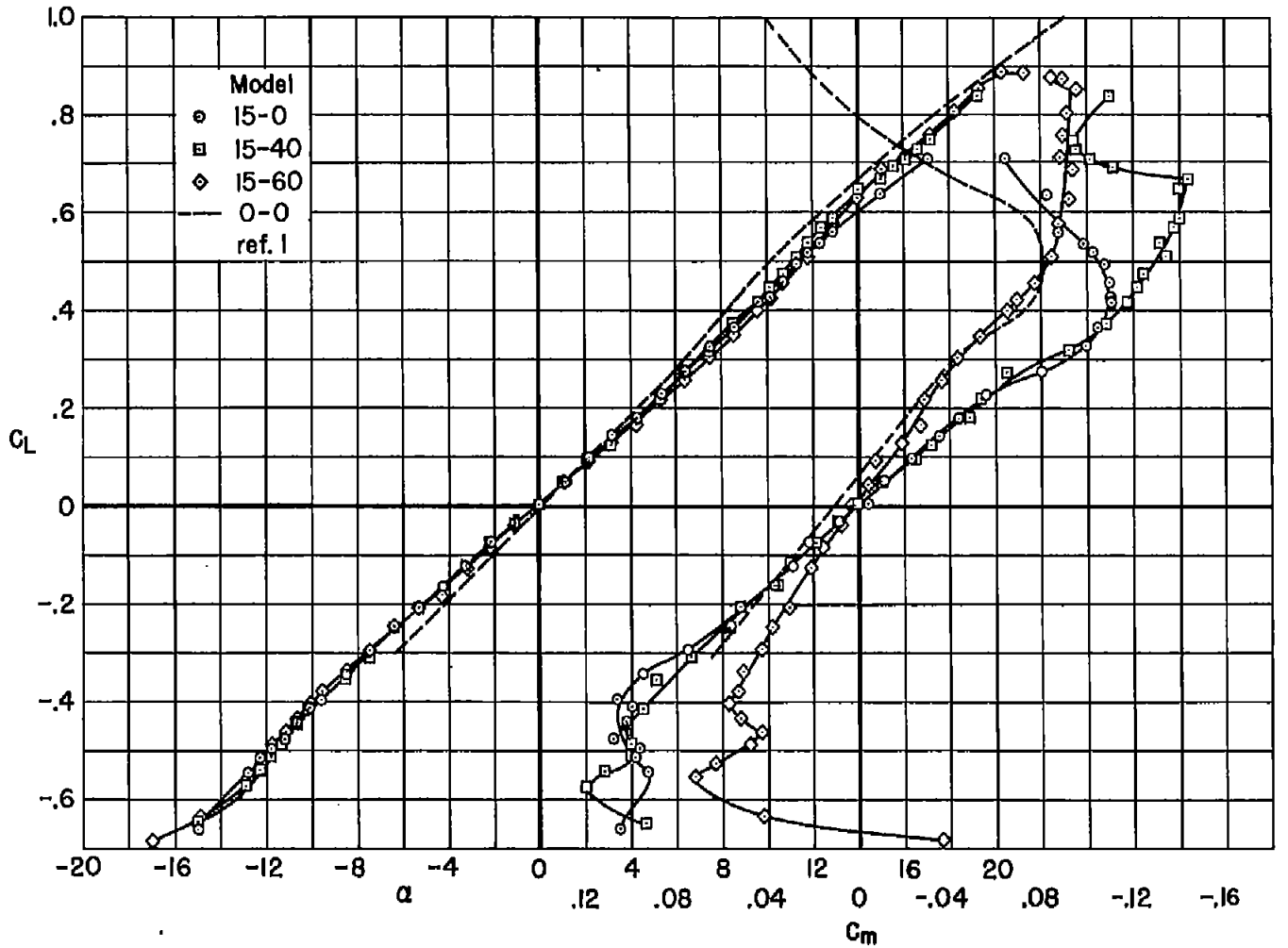

(a) Lift and pitching moment.

Figure 5.- Lift, pitching-moment, and drag characteristics of the abrupt-droop models.

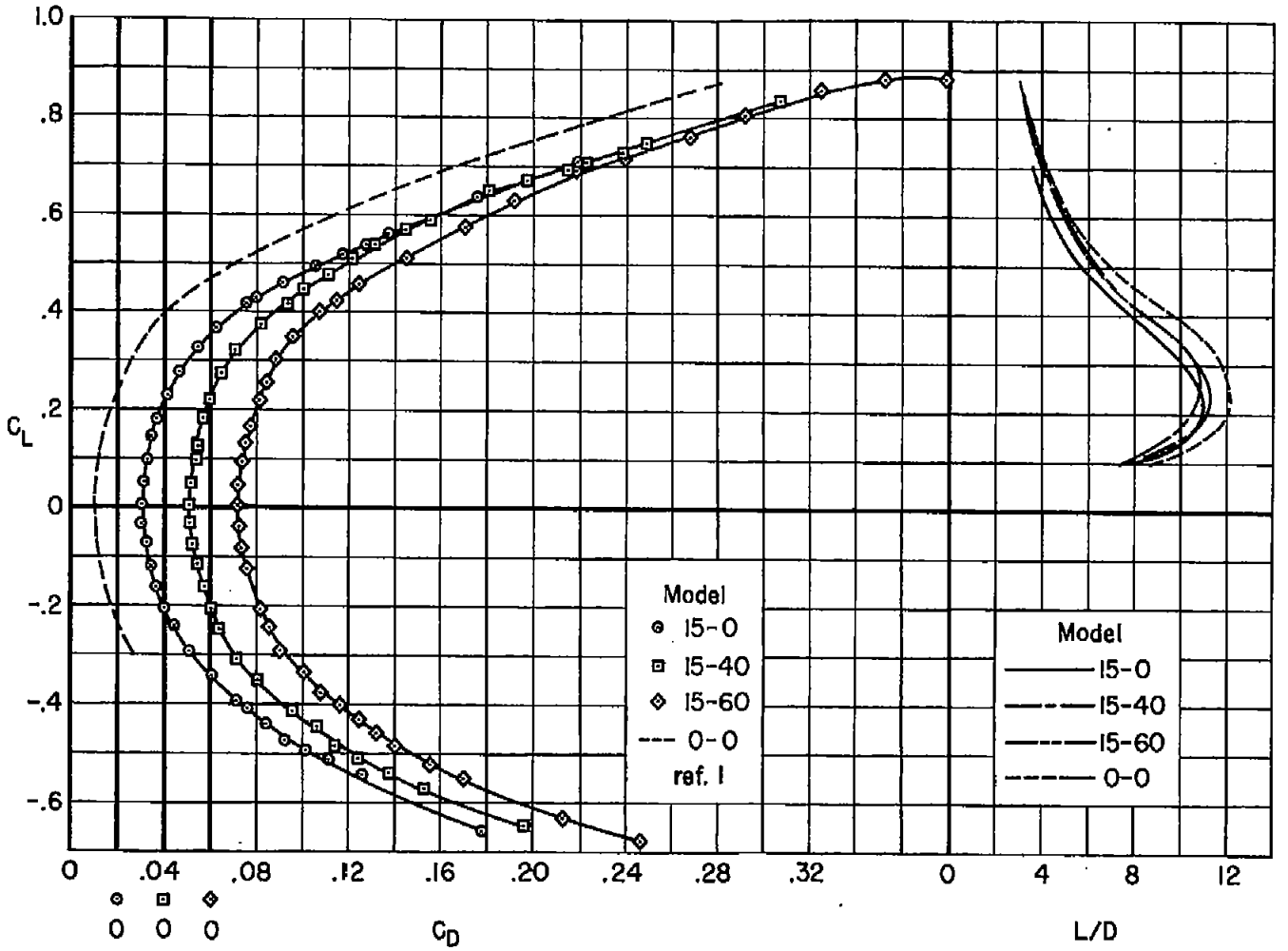

(b) Drag and lift-drag ratio.

Figure 5.- Concluded.

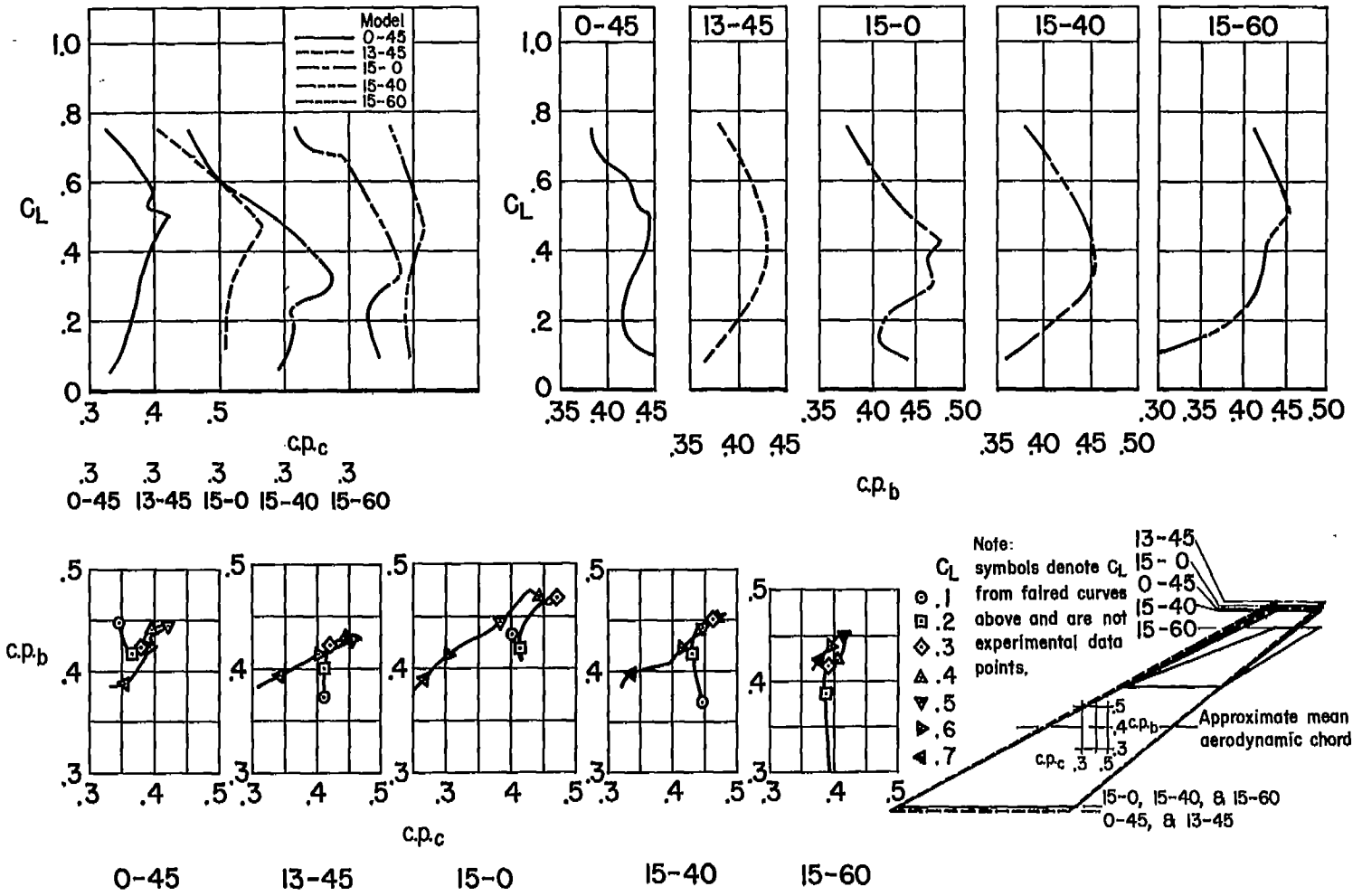

Figure 6.- Center-of-pressure movement on the models.

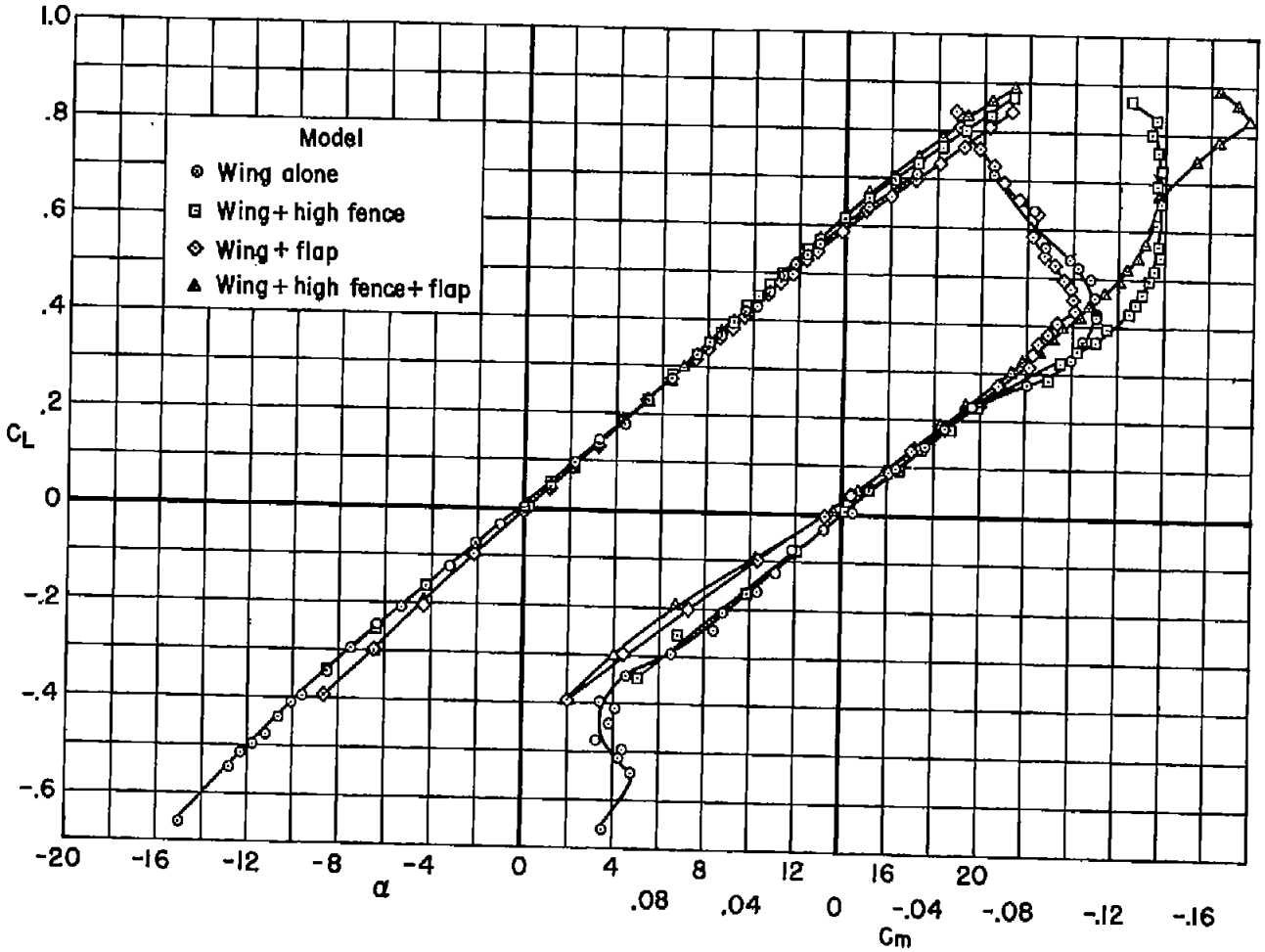

(a) Lift and pitching moment.

Figure 7.- Comparison of the effects of the fence and of the leading-edge flap on the characteristics of model 15-0.

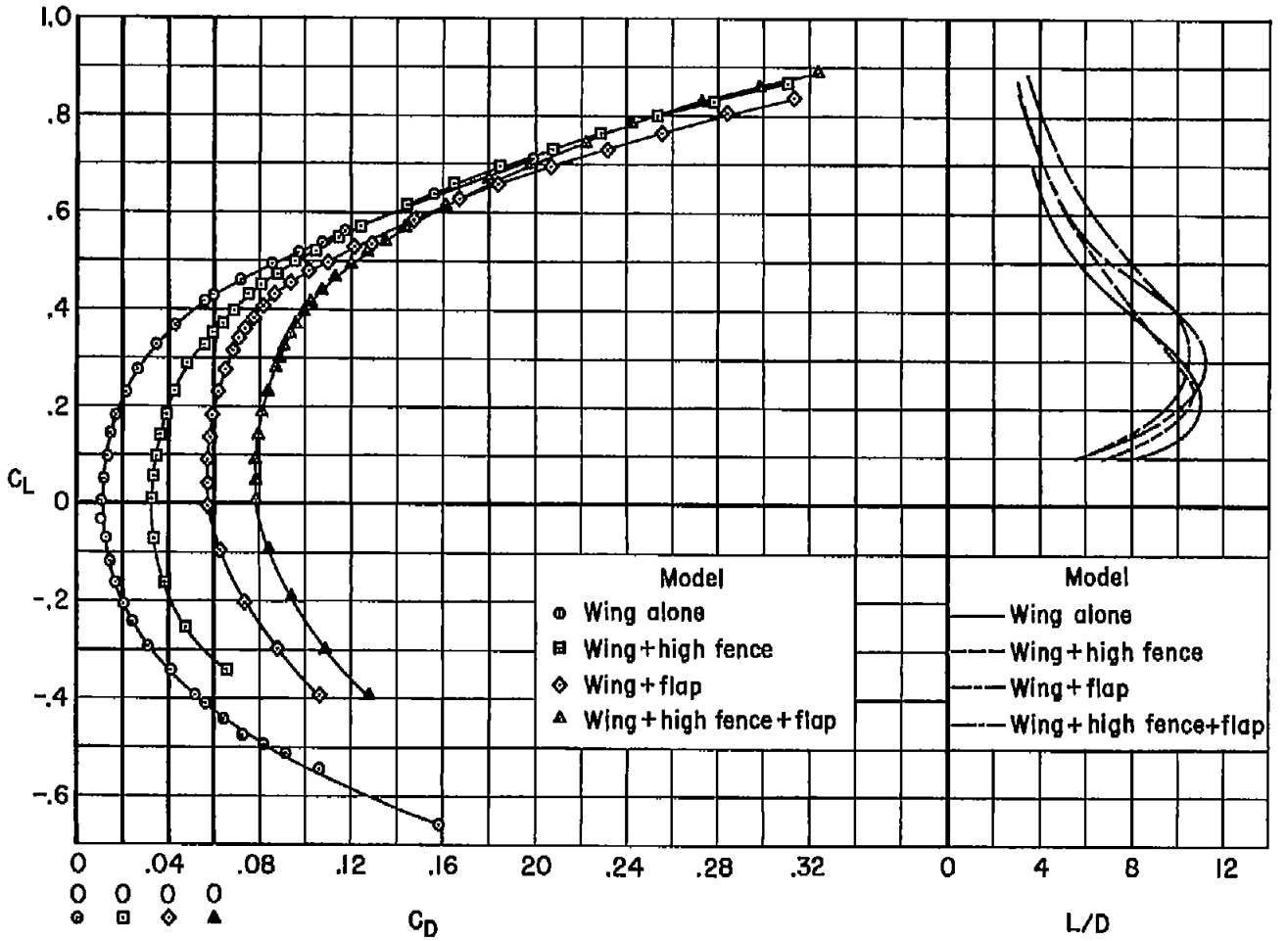

(b) Drag and lift-drag ratio.

Figure 7.- Continued.

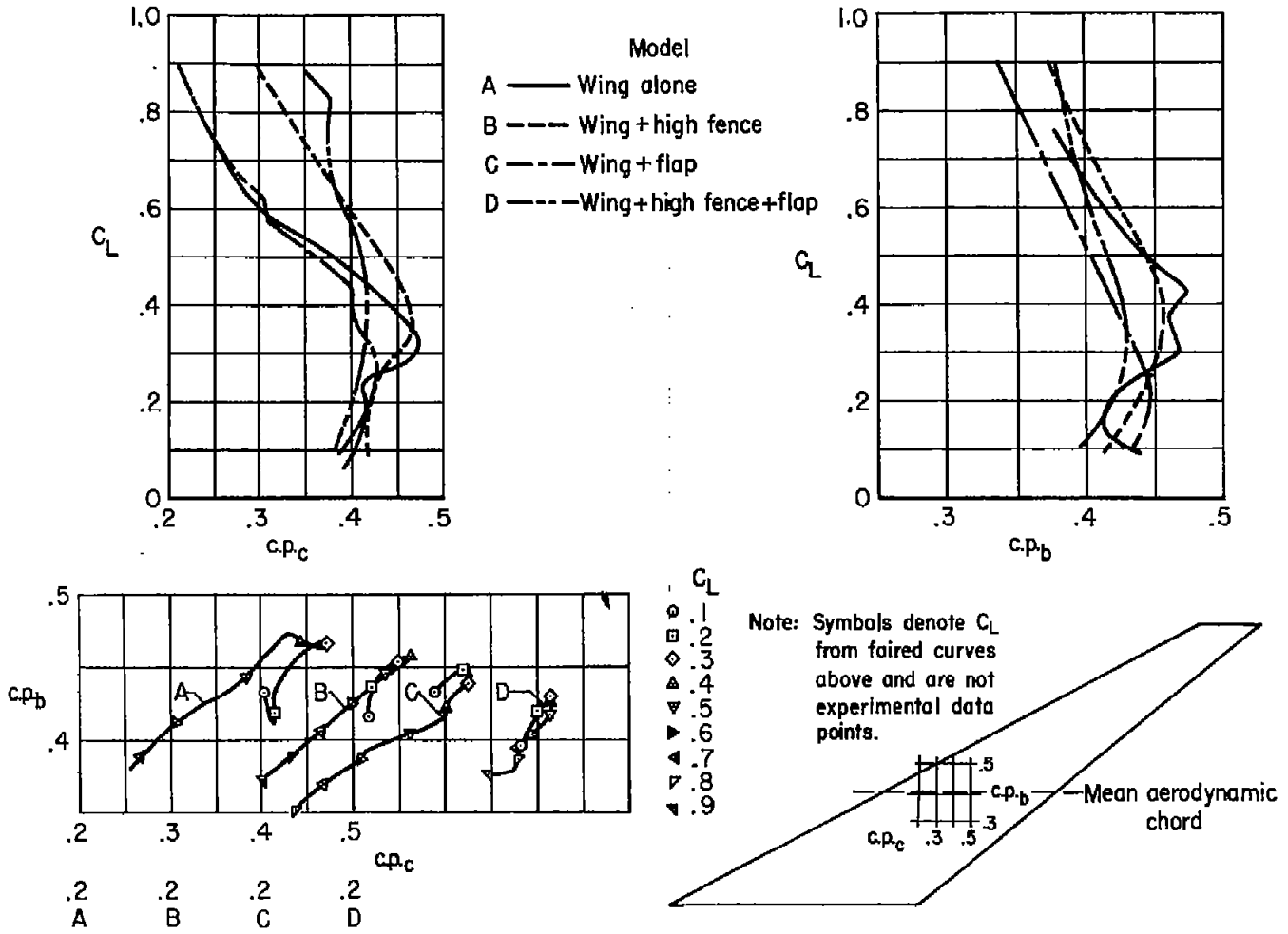

(c) Center-of-pressure movement.

Figure 7.- Concluded.

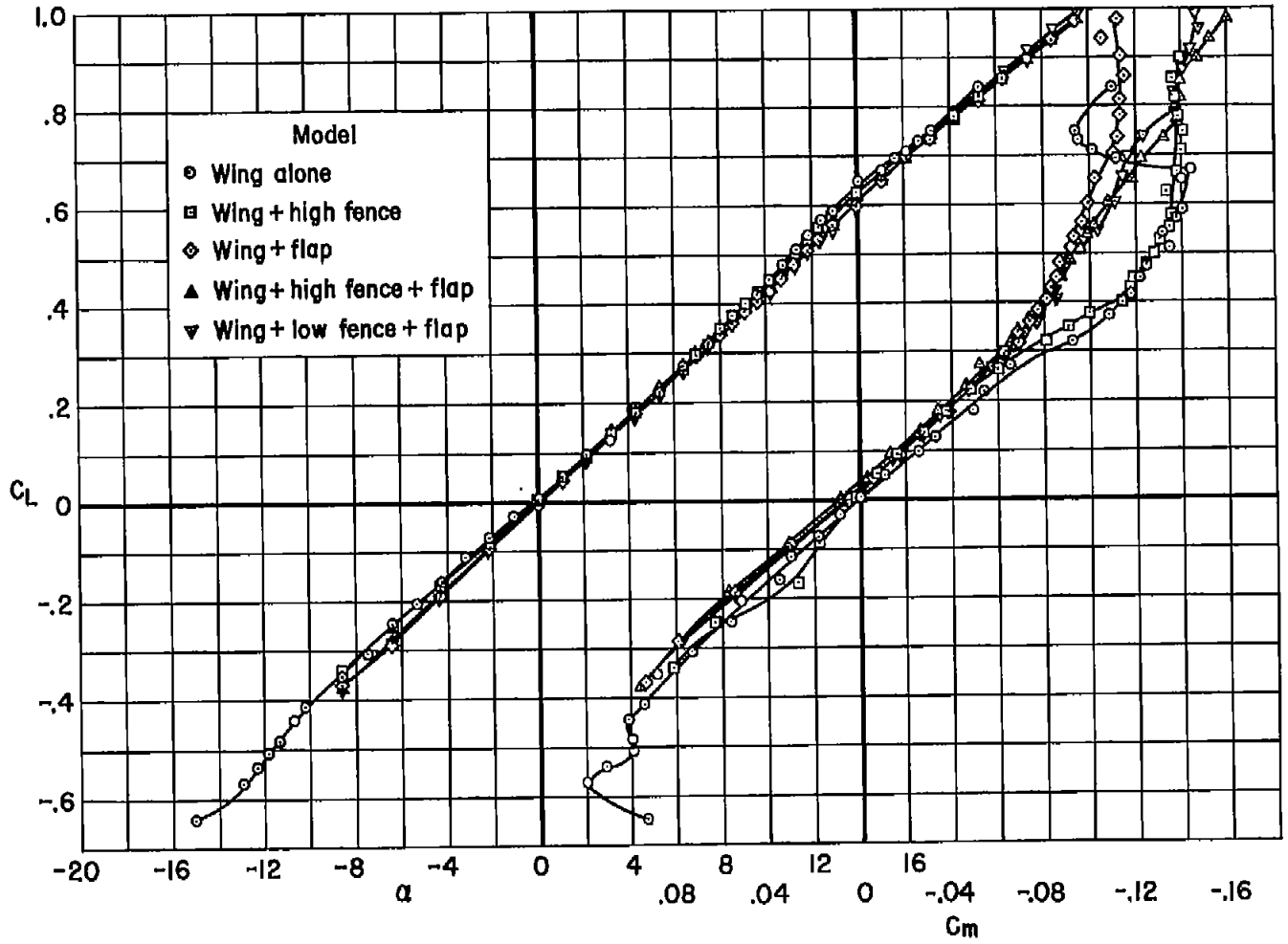

(a) Lift and pitching moment.

Figure 8.- Comparison of the effects of the fences and of the leading-edge flap on the characteristics of model 15-40.

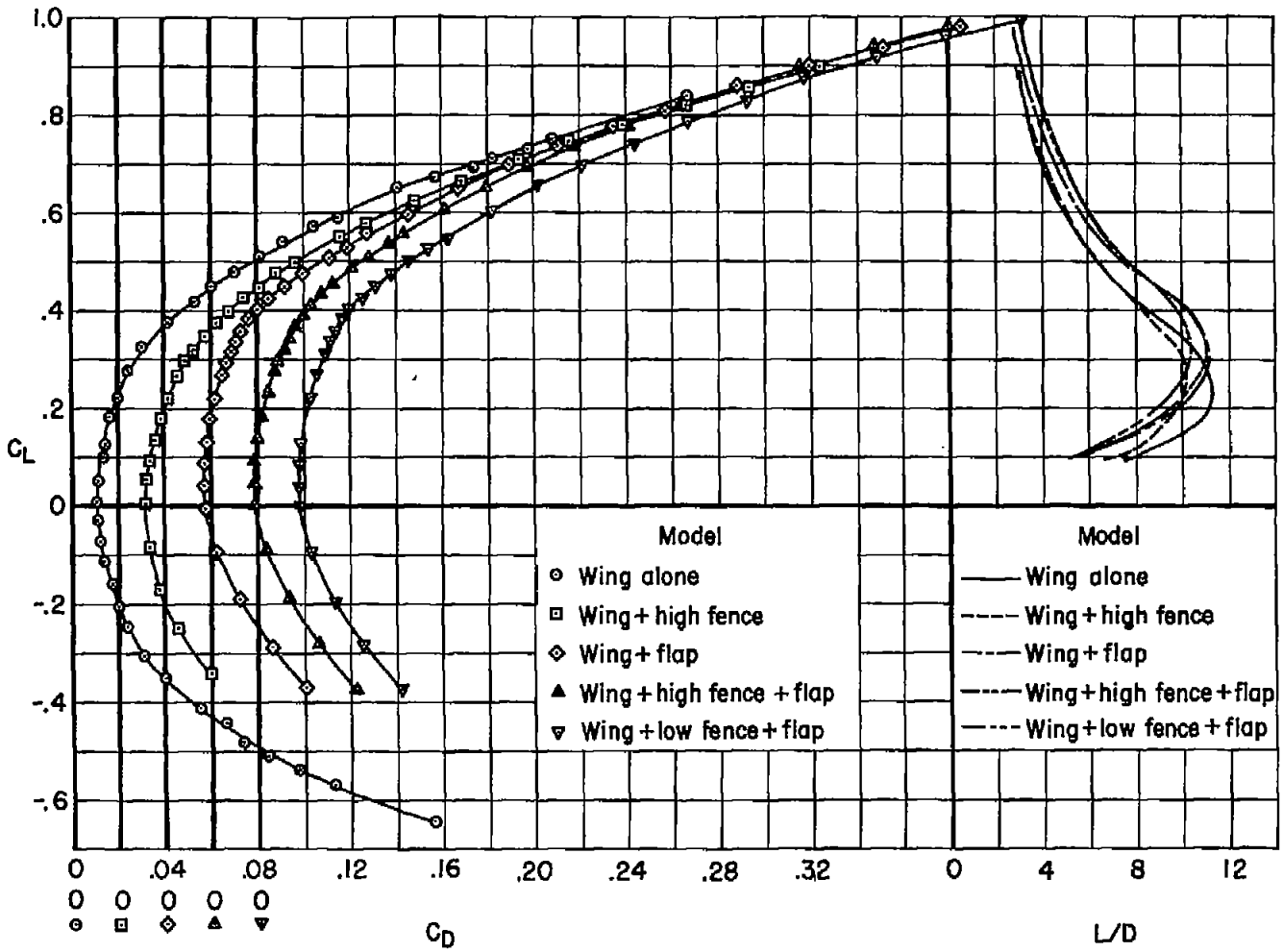

(b) Drag and lift-drag ratio.

Figure 8.- Continued.

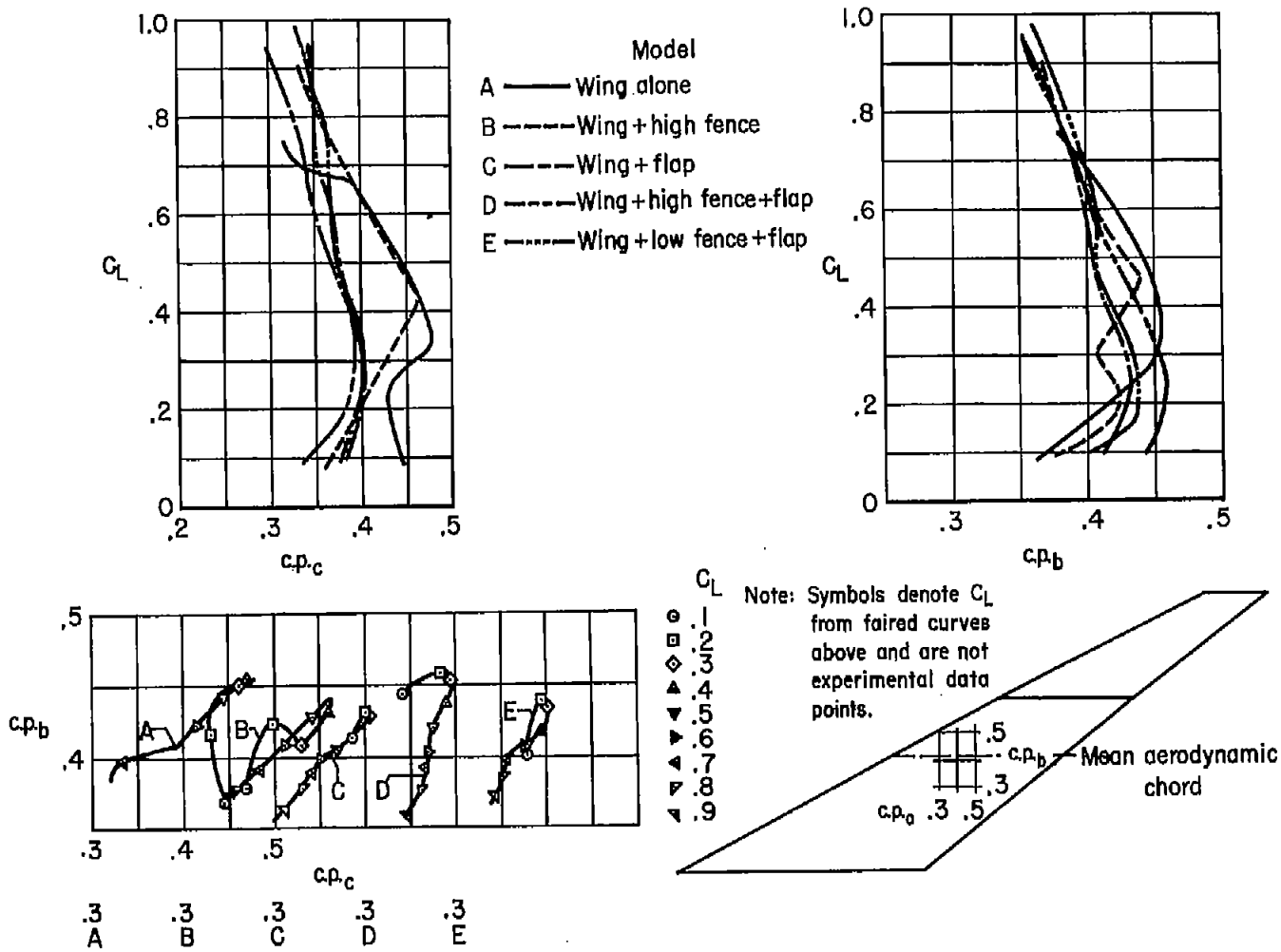

(c) Center-of-pressure movement.

Figure 8.- Concluded.